Dynamic Characteristics of a Hollow Femur

B.W. Huang[1,2], C.H. Chang[3], F.-S. Wang[4], A.D. Lin[1], Y.C. Tsai[1], M.Y. Huang[1], J.-G. Tseng[2]*

[1]Graduate Institute of Mechatronics Engineering, Cheng Shiu University, Taiwan, ROC
[2]Medical Mechatornics Engineering Program, Cheng Shiu University, Taiwan, ROC
[3]Neurosurgery department, Mackay Memorial Hospital Taitung Branch, Taiwan, ROC
[4]Kaohsiung Chang Gung Memorial Hospital, Center for Laboratory Animals, Taiwan, ROC
*E-mail: james.tseng@csu.edu.tw. (NSC 99-2632-E-230-001-MY3)

Abstract: The femur is the largest, longest, and strongest bone of the human skeleton and has the ability to support up to 30 times the weight of an adult. This paper examines the fundamental dynamic characteristic of both the solid and hollow femur, experimentally and numerically. Reverse engineering is applied to obtain the outer geometry of synthesis femur. Noble's Canal Flare Index (CFI) is applied to excavated marrow material of the femur canal and to build a more realistic human hollow femoral model. Both solid and hollow femur are imported to the finite element package, ANSYS, to perform the analysis. The mechanical properties of real human femur are substituted into the FE model to achieve the final goal of finding dynamic response of human solid and hollow femur. The comparison of natural frequencies, stress, strain, and displacement of both solid and hollow femur are matched to the physical rules.

Keywords: Human Hollow Femur, Geometry, Femoral Canal, Reverse Engineering

1. Introduction

The femur, or thigh bone, extending from the hip to the knee, is the most proximal bone of the leg in vertebrates capable of walking or jumping. The femur is the largest, longest, and strongest bone of the human skeletons. Its rounded, smooth head fits into a socket in the pelvis called the acetabulum to form the hip joint. The head of the femur is joined to the bone shaft by a narrow piece of bone known as the neck of the femur. The neck of the femur is a point of structural weakness and a common fracture site. The lower end of the femur hinges with the tibia (shinbone) to form the knee joint.

Many studies have focused on geometry, biomechanical properties, fractural type, etc. of a human femur [1~6]. A typical femur structure includes compact bone, sponge bone, medullary cavity, yellow marrow, periosteum, articular cartilage, etc, as shown in Fig. 1 [7]. The average adult male femur is 48 centimeters in length and 2.84 cm in diameter at the mid-shaft, and has the ability to support up to 30 times the weight of an adult. Yan et al. measure the parameters of femur from 52 normal adults' X-ray photograph. The total length of femur medullary cavity of male and female are 33.51±0.63 cm and 33.13±0.64 cm, respectively. The length of the narrow point are 5.61±0.49 cm (male) and 5.17±0.46 cm (female). The narrowest parts are located on the proximal end of medullary cavity and the distance of them are 3.55±0.15 cm (male) and 3.52±0.27 cm (female). The sagittal diameter is longer than the coronal diameter of the narrow point of the medullary cavity [8].

Ho Bo Tho models bone and joints with individualized geometric and mechanical properties derived from medical images [9]. Brekelmans et al. [10], proposed the finite element method (FEM) to analyze the mechanical behavior of skeletal structure, and built a 2D FEM models of the femur (226 triangular elements and 146 nodes) in 1972 which showed roughly the development and transmission of stress and marked the beginning of FEM applied to the orthopedic biomechanics. Gross et al [11], build a hollow femoral stem by the hexahedral elements of ANSYS software and discuss the stress shielding effect. Yerry and Shephard [12] propose the Octree method to create three-dimensional finite element model which more able to show the true dynamic behavior of femur. Taylor et al. [13] estimated the orthogonal bone material properties through modal experiments and ultrasound bone density measurements, and then verify the results with Finite Element Analysis (FEA). Zhang et al [14], construct a 3D FE model which solid elements are used to model bone, soft tissue and the lining. On the other hand, contact elements are employed to simulate the interface of bone and internal lining to get more realistic dynamical behavior at the interface. Kleemann et al [15], discuss Total Hip Arthroplasty (THA) loading arising from increased femoral anteversion and offset may lead to critical cement stresses. Noble [16, 17] measures 200 femurs and defines a method called canal flare index (CFI) to scan the shape of the proximal femoral canal. CFI is the ratio of the canal width, 20 mm above lesser trochanter, to the canal width in the middle of diaphysis. Noble classifies the canal into three types: stove pipe (CFI<3), normal (3<CFI<4.7), champagne-fluted (CFI>4.7). Stephen and Eckrich [18] propose the relationship between femoral dimensions and its rotation under X ray.

In reverse engineering field, Song and Kim [19] propose an autonomous digitization of free-form surface on a CNC coordinate measuring machine. Kruth and Kerstens [20] establish a free surface from limited boundary conditions of point database. These geometric boundary conditions are then merged into a CAD model according to NURBS theory and to form a free surface model [21]. Peng and Loftus [22] propose an integrated photometric stereo photography illumination algorithm to reconstruct the three-dimensional surface.

This research employs reverse engineering, Noble CFI method and FEM to obtain the outer geometry, to excavate the cancellous bone according to inner canal shape, and to mesh the model of the hollow femur. The results are compared with Liang's outcome which is focused on solid femur [23].

2. Methodology

The flow chart of this research is shown Figure 2. First, it employs reverse engineering by using 3D white light scanner to obtain the outer profile of a teaching synthesis femur (made by plastic material).

The repair software, Studio, is used to patch the holes on the scanned 3D femur diagram which is then imported into finite element analysis software ANSYS [24]. The simulation results are verified with the experimental data to make sure the accuracy of the FEM model.
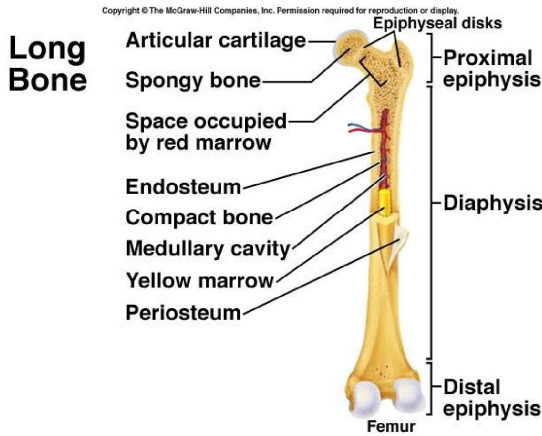
Figure 1. Schematic diagram of the femur structure (source: http://dc260.4shared.com/doc/lQlSf0m5/ preview.html) [7]
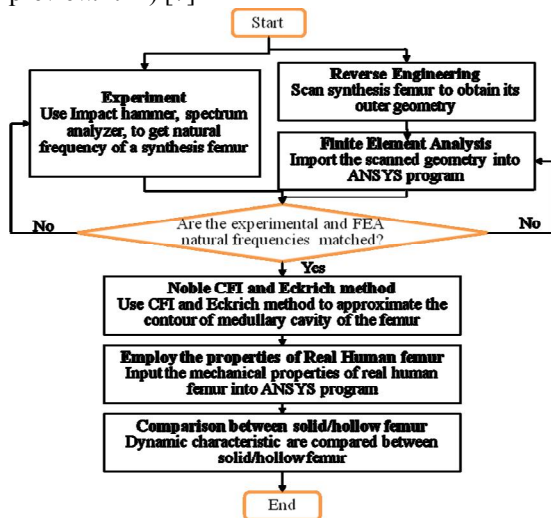
Figure 2. Flow chart of this research
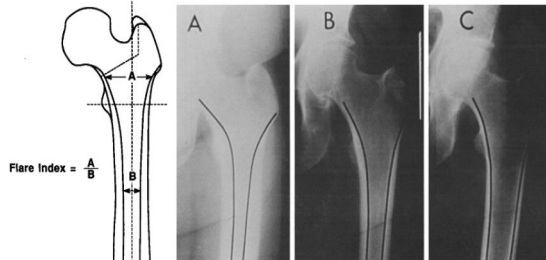
Figure 3. Proximal femur bone marrow cavity shape scanning method [25]

Proximal medullary cavity shape of the femur is sketched by Noble's CFI method. The femur is classified into three types (as shown in Figure 3): (A) Chimney-type (stovepipe) (CFI is less than 3), (B) normal type (CFI is between 3 to 4.7), and (C) inverted champagne-type (champagne-flute) (CFI is greater than 4.7). The cancellous bone and marrow are then cut off by drawing technique according to the above obtained the profile of femoral canal.
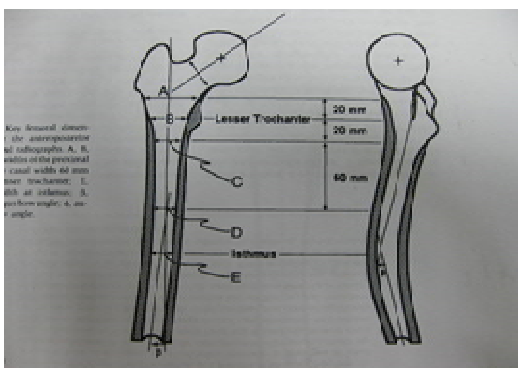
Figure 4. The relationship between femoral canal dimension and rotation [18]

Since Young's modulus of cortical bone is from dozens to hundred times higher than cancellous bone [9] and even much higher than the marrows, this hollow femur model contains only compact bone, the marrow are cut off. It is then analyzed in ANSYS program with the mechanical properties of real human femur. Hollow femoral model is very important to much accurately simulate real human femur. The dynamic characteristic of real human hollow femur is obtained and is compared with the solid femoral model.

3. Femoral canal contour drawing process

According to radiographic appearance of the femoral canal proposed by Eckrich et al., A is the canal width 20 mm above lesser trochanter, B is the canal width at lesser trochanter, C is the canal width 20 mm below lesser trochanter, D is the canal width 60 mm below lesser trochanter, E is the canal width at isthmus of the femur, β is the angle between vertical line passing through D and center line parallel to femoral canal below D, φ is the angle between upper and lower line parallel to the upper and lower femoral canal, respectively, cross at isthmus and measured in the side view of the femur, as shown in Figure 4. The calculated CFI value is 3.07 of the proposed femoral model which is normal type femur. Assume canal width A at front view is 40 mm and side view is 30 mm, then use the angle β and φ, arithmetical progression, and CFI value to calculate each point from A to E and the corresponding canal width of the distal (lower part) femur, as shown in Table 1.

Table 1. Dimensional of femoral canal

Item	Front view		Side view	
	Parameters	Value	Parameters	Value
Angle	β	0.1±0.3º	φ	7.9±0.6º
Canal width	A	40 mm	A	30 mm
	B	30.31 mm	B	24.07 mm
	C	20.1 mm	C	20.1 mm
	D	15.66 mm	D	17.8 mm
	E	13 mm	E	17.34 mm
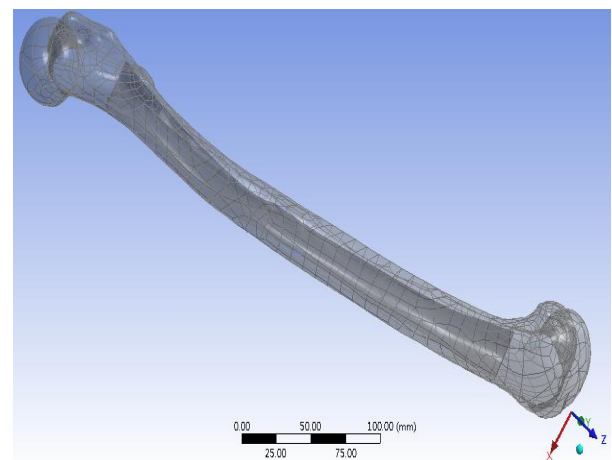
Figure 5. Hollow femoral model
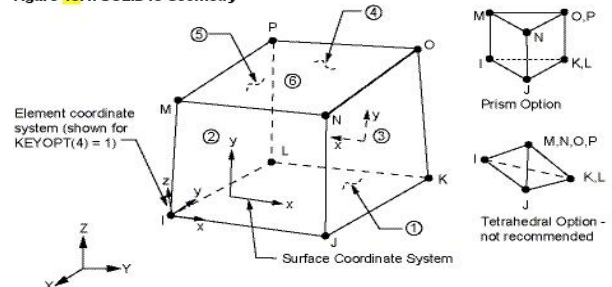
Figure 6. ANSYS Solid45 element

According to the above Table 1., the hollow femur model is built as shown in Figure 5.

4. Finite Element Analysis

ANSYS provides different type of elements,

724

such as point element, line elements, surface elements and body elements, etc. All the elements are selected according to the construction of the graph and the solution needed for the analysis [27, 28]. ANSYS higher order 3-D, 8-node solid element SOLID45 (Figure 6), suitable for irregular grid, is chosen for this hollow femur model.

There are free mesh and mapped mesh in ANSYS. In free mesh, solid models requires not much, just to specify mesh size, density and type, then use the Mesh Generator to produce grid. However, the mapped mesh is more stringent. To meet a certain requirements in a complex geometric will spend a lot of time for detail cutting to complete the entire grid.

Nevertheless, the mapped mesh will turn out more rigorous and accurate results. Finer grid means more elements to be analyzed and will need longer process time. This study uses mapped mesh to form the finite element model, as shown in Figure 7.

The mechanical properties of the homogenous, isotropic synthesis femur (Polyethylene) are: Young's modulus: 1.3 GPa, density, 950 kg/m3, and poisson's ratio: 0.42. The mechanical properties of real human femur (assume homogenous and isotropic material) are used according to Hsu's result [26]: Young's modulus: 17 GPa, density, 2132.6 kg/m3, and poisson's ratio: 0.3.

5. Results and Discussions

Convergence test is performed before doing further investigation. The fundamental natural frequency is converged when the hollow femoral model is divided into 18,000 elements. Therefore, more than 30000 elements are used to simulate the hollow femoral model.

After the several lower natural frequencies of FEM model are matched with experimental results, the material properties of real human femur are substitute into the FEM model. Both solid femoral model and hollow femoral model are conducted for the analysis. The vibration natural frequencies of these two models are compared and shown in Table 2.
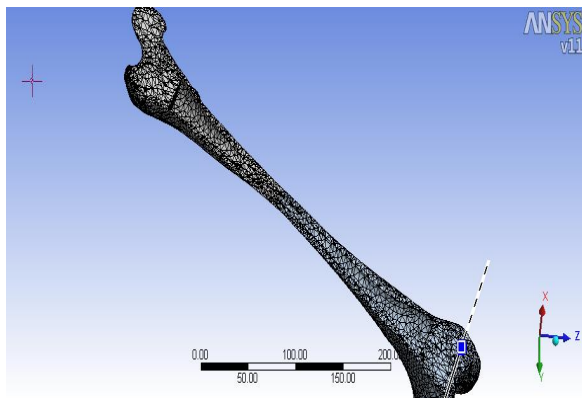
Figure 7. ANSYS meshed hollow femur model

Table 2. Natural frequency comparison between solid and hollow femoral model

Mode	Frequency (Hz)		Difference Value(%)
	Solid femur	Hollow femur	
1	265.53	271.85	-2.38
2	286.91	291.11	-1.46
3	609.21	564.08	7.41
4	881.44	901.55	-2.28
5	926.71	957.18	-3.29

Table 3. Stress, strain, displacement comparison between solid and hollow femoral model when apply a force of 1000N

Item	Solid femur	Hollow femur	Difference Value
Stress	40.613 Mpa	42.741 Mpa	2.128 Mpa
Strain	0.00239	0.00251	0.00012
Displacement	5.15 mm	8.66 mm	3.51 mm

The natural frequencies of hollow femur are basically higher than solid femur, since the moment of inertia of hollow femur is higher than that of solid femur and the mass of hollow femur is lower than that of solid femur. When apply 1000N force on the distal part of both solid and hollow femur and the response stress, strain, and displacement at the same place is shown in Table 3. The stress, strain and displacement of a solid femur are lower than that of the hollow femur. Because stress (σ), moment of inertia (I), moment of cross section (M), and distance with neutral axis (y) in bending motion have the relationship: $\sigma=(M*y)/I$. Therefore, σ is inverse proportional to I, and σ is proportional to ε(strain). In other words, I is the ability of an object to resist deformation, also is the stiffness of the object. The greater value of the moment of inertial (I), the harder of the material to be deformed. The first mode shapes of both solid and hollow femur are shown in Figure 8 and 9, respectively.

7. Conclusion

The numerical simulation of synthesis femur, solid human femur, hollow human femur, and experiments of the synthesis femur are investigated in this study. The major conclusions drawn from the this study are summarized as follows:
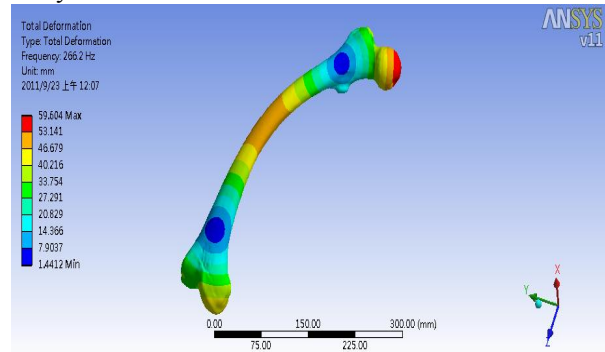
Figure 8. First mode shape of a solid femur (266Hz)
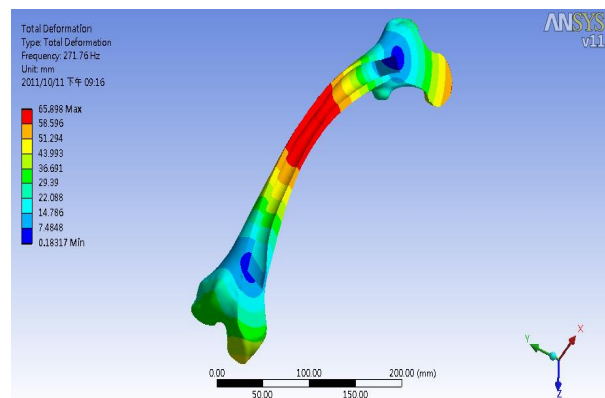
Figure 9. First mode shape of a hollow femur (272Hz)

(1) Both FEA and experimental results are quite match for a synthesis femur. Therefore, the outer geometry femur model is confirmed and can be used to calculate the dynamic properties of the real human femur.

(2) The drawing process of excavation the femur canal is built up to much approximate real human hollow femur situation.

(3) The natural frequencies, stress, strain, and displacement when apply a 1000N force are compared between the solid and hollow femur. All of them are matched with the physical rules.

(4) The advantage of this method is to avoid analyze the fresh or dry human bones and still can get quite promising results.

Acknowledgement

Corresponding Author:
Jung-Ge Tseng, Ph.D.
E-mail : james.tseng@csu.edu.tw

References
1. N. Hraiech, C. Boichon, M. Rochette, T. Marchal, M. Horner, "Statistical Shape Modeling of Femurs Using Morphing and Principal Component Analysis," ASME J. Med. Devices, Vol. 4 (2), 027534, 2010.
2. Y. Jun and K. Choi, "Design of patient-specific hip implants based on the 3D geometry of the human femur," Advances in Engineering Software, Vol. 41, pp. 537–547, 2010.
3. M. Peacock, K.A. Buckwalter, S. Persohn, T.N. Hangartner, M.J. Econs, S. Hui, "Race and sex differences in bone mineral density and geometry at the femur," Bone, Vol. 45, pp. 218–225, 2009.
4. J. Panula, M. Sävelä, P.T. Jaatinen, P. Aarnio, S.-L. Kivelä, "The impact of proximal femur geometry on fracture Type – a comparison between cervical and trochanteric fractures with two parameters," Scandinavian Journal of Surgery, Vol. 97, pp. 266–271, 2008.
5. Z. Chen, T.J. Beck, J.A. Cauley, C.E. Lewis, A. LaCroix, T. Bassford, G. Wu, D. Sherrill and S. Going, "Hormone therapy improves femur geometry among ethnically diverse postmenopausal participants in the Women's Health Initiative hormone intervention trials," J. Bone Miner Res. 23(12), pp.1935-45, 2008.
6. C.S. Duncan, C.J.R. Blimkie, A. Kemp, W. Higgs, C.T. Cowell, H. Woodhead, J.N. Briody, and R. Howman-Giles, "Mid-femur geometry and biomechanical properties in 15- to 18-yr-old female athletes," Official Journal of the American College of Sports Medicine, Medicine & Science in Sports & Exercise, pp. 673-681, 2002.
7. Schematic diagram of the femur structure, source: http://dc260.4shared.com/doc/lQlSf0m5/preview.html
8. H. Yan, J. Zhang, K. Liu, K. Wang, "Morphological study of the femur medullary cavity and its significance," Journal of Xi'an Jiaotung University (Medical Sciences), Vol. 27, No. 3, pp. 236-239, 2006.
9. MC. Ho Bo Tho, "Bone and joints modelling with individualized geometric and mechanical properties derived from medical images," CMES, Tech Science Press, Vol. 4, no.3&4, pp.489-496, 2003.
10. W. Brekelmans, H. Poort, T. Slooff, "A new method to analysis the mechanical behavior of skeletal parts," Acta Orthop Scand, 301-317, 1972.
11. S, Gross, E.W. Abel, "A finite element analysis of hollow stemmed hipprostheses as a means of reducing stress shielding of the femur," Journal of Biomechanics, Vol. 34, pp. 995-1003, 2001.
12. M.A. Yerry and M.S. Shephard, "Automatic three-dimensional mesh generation by the modified-octree technique", International Journal for Numerical Methods in Engineering, Vol. 20, pp.1965-1990, 1983.
13. W.R. Taylor, E. Roland, H. Ploeg, D. Hertig, R. Klabunde, M.D. Warner, M.C. Hobatho, L. Rakotomanana, S.E. Clift, "Determination of orthotropic bone elastic constants using FEA and modal analysis", Journal of Biomechanics, Vol. 35, pp. 767-773, 2002.
14. M. Zhang, "Development of a non-linear finite element modelling of the below-knee prosthetic socket interface," Medical Engineering & Physics, Vol. 17, pp. 559-566, 1995.
15. R.U. Kleemann, M.O. Heller, U. Stoeckle, W.R. Taylor, and G.N. Duda, "THA loading arising from increased femoral anteversion and offset may lead to critical cement stresses", J. Orthop. Res., Vol. 21, pp. 767-774, 2003.
16. PC Noble, JW Alexander, U. Lindahl, "The anatomic basis of femoral component design," Clin. Orthop. Vol. 235, pp. 148-65, 1988.
17. PC Noble, E Kamaric, N Sugano, Matsubara Ma, Harada Y, Ohzono K, Paravic V, "Three-Dimensional Shape of the Dysplastic Femur: Implications for THR," Clin Orthop Vol. 417, pp. 27-40, 2003.
18. S. G.J. Eckrich, PC. Noble, H.S. Tullos, "Effect of rotation on the radiographic appearance of the femoral canal, Original Research Article," The Journal of Arthroplasty, Vol. 9 (4), pp. 419-426, 1994.
19. C. K. Song and S. W. Kim, "Reverse Engineering : Autonomous Digitization of Free-form Surface on A CNC Coordinate Measuring Machine," Int. J. Math. Tools Manufact, Vol. 37, pp. 1041-1051, December, 1997.
20. J. P. Kruth, A. Kerstens, "Reverse engineering modeling of free-form surfaces from point clouds subject to conditions", Journal Materials Processing Technology Vol.76, pp. 120-127, 1998.
21. Jeng-Nan Lee and Kuan-Yu Chang, "An Integrated Investigation of CAD/CAM for the Development of Custom-made Femoral Stem," Life Science Journal, Vol 7, No 1, 56 – 61, 2009.
22. Q. J. Peng, M. Loftus, "A new approach to reverse engineering based on vision information," International Journal of Machine Tools & Manufacture Vol.38, pp. 881-899, 1998.
23. S.H. Liang, An Investigation on Dynamic Characteristics of a Human Leg Bone, Master Thesis, Institute of Mechatronics Engineering, Cheng Shiu University, 2011.
24. B.W. Huang, H.K. Kung, K.Y. Chang, P.K. Hsu, J.-G. Tseng, "Human Cranium Dynamic Analysis," Life Science Journal, 6(4): 15– 22, 2009.
25. Y.E. Lee, "The Proximal Femoral Canal Geometry of Osteoporosis, Osteoarthritis, and Osteonecrosis," Master Thesis, Institute of Biomedical Engineering , National Yang Ming University, 2005.
26. J.-T. Hsu, C.-H. Chang, S.-I Chen, "Investigate the influence of material properties under various loading mode: finite element simulations," Engineering Science and Chinese-Western medical Application Conference, 2002.
27. Y.K. Tu, Y.Y. Hong, Y.C. Chen, "Finite element modeling of kirschner pin and bone thermal contact during drilling," Life Science Journal, 6(4): 23-27, 2009
28. Chang Kuan Yu, Chang Hong Chang, Yu Pu Ping, Yen Ke Tien, Huang Bo Wun, "Natural Properties in a Micro Drill Cutting into Bones," Life Science Journal, 6(4): 28–33, 2009.

2/1/2012